Multi-Temporal SAR Change Detection using Wavelet Transforms

Nizar BOUHLEL
Agrocampus-ouest Angers
UMR INRAe IRHS
Angers, France
nizar.bouhlel@agrocampus-ouest.fr
https://orcid.org/0000-0002-4861-8550

David ROUSSEAU
University of Angers,
LARIS, UMR INRAe IRHS
Angers, France
david.rousseau@univ-angers.fr

***Abstract*—In this paper, we propose a new method for automatic change detection in multi-temporal SAR images based on statistical wavelet subband modeling. The proposed method allows to take into account the correlation structure between subbands by modeling the wavelet coefficients through multivariate probability distributions. Two types of correlation are investigated: inter-scale dependence and inter-orientation dependence. The multivariate Gaussian distribution is used to model the interdependencies between wavelet coefficients at different orientations and scales. Kullback-Leibler similarity measures are computed and used to generate the change map. We show that the information residing in the correlation between subbands improve the accuracy of the change map and lead to better performance.**

***Index Terms*—Change Detection, Kullback-Leibler (KL) divergence, Multivariate Gaussian distribution, Multi-temporal synthetic aperture radar (SAR) images, Wavelet Transform, Subband dependence.**

I. Introduction

Change detection in remote sensing becomes very important for environmental monitoring [1], [2], damage assessment [3], land cover dynamics, analysis of urban changes [4], agricultural surveys [5], analysis of forest or vegetation changes [6], [7]. Synthetic aperture radar (SAR) sensors are widely used for change detection [8], [9]. They can provide high resolution multi-temporal images, at short intervals and during complete seasonal cycles. Change detection is a process that analyzes a pair of SAR images of the same geographic area acquired at different times and identifies eventual changes. The result is a generation of a change detection map in which changed area are explicitly identified.

Change detection in multitemporal single-polarization SAR images is usually carried out in an unsupervised way since the ground truth is usually unavailable. Unsupervised change detection consists to discriminate between two classes, namely changed and unchanged classes, without any prior information. Generally, after pre-processing the SAR images (geometric correction, co-registration, speckle filtering), the unsupervised change detection performs by comparing some features of the two images by using some similarity metrics resulting in a change map, and then a threshold is applied to produce two classes associated with changed and unchanged pixels.

In the literature, several unsupervised change detection approaches have been proposed and can be classified in two groups: methods based on pixel intensity and methods based on local statistics [10]. The first one is based on the pixel intensity and the neighboring of the pixel. They include image differentiating, mean ratio/log-ratio measures [11], [12], Gauss log-ratio [13], etc. The second one uses the local statistics estimated by considering some local probability density functions (pdfs) of the neighborhood of homologous pixels of the pair of images used for the change detection. These distributions have been chosen particularly to model adequately the statistics of SAR images. Once the parameters of the chosen distribution are estimated, their comparison can be performed using different criteria and the most usual one is the Kullback-Leibler divergence (KLD) [14], [15]. For the final step of the change detection process, the decision threshold is selected to produce binary change detection map. Several methods have been proposed to determine the best threshold value in a completely unsupervised manner: to name a few of them, CFAR algorithm [16], Otsu's method [17], Kittler and Illingworth (K&I) algorithm [18].

Standard pdf based change detection methods focus on univariate models. These models are relevant for detecting changes in homogeneous areas. However, these models lack in capturing changes near edges or textures. Wavelet transform is a powerful modeling tool that can lead to performant texture modeling and change detection. Indeed, texture can be easily represented and discriminated in wavelet domain [21]. Wavelet transform is used to decompose the image into multiscale oriented subbands that are sensitive to horizontal, vertical and diagonal edges. In the community of multi-temporal SAR change detection, several works on statistical wavelet subband modeling have been developed based on univariate models. Indeed, wavelet coefficients have been modeled as independent Gaussian variable or as jointly Gaussian vectors [19]. Recently, non-Gaussian distributions of the wavelet subband coefficients are frequently used. In fact, the generalized Gamma distribution (GΓD) [20], [21] and the generalized Gaussian distribution (GGD) [22], [21] are suitable to model the wavelet coefficient magnitudes of each subbands, since they are more peaked and heavy-tailed than the Gaussian distribution [23]. Closed-form expression of Kullback-Leibler divergence for both GGDs and GΓDs are given in the literature to assess the similarity [21], [14], [20].

Generally, the subbands are assumed to be independent and no dependence across wavelet orientations and scales are modeled. But this dependence exists and it can be employed to provide better accuracy in the similarity measure. To the best of our knowledge, few works have been developed in the literature aiming to take into account the correlation. In [24], author studied the correlation properties of wavelet transform coefficients at different subbands and resolution levels, applying these properties on an image coding scheme based on neural networks. In [25], a joint alpha-stable sub-Gaussian distribution was used to model dependence across wavelet orientations and scales for texture retrieval. Good results have been obtained, but a computationally complex gaussianization step was required.

In this paper, a change detection method based on wavelet coefficient magnitude modeling is proposed to take into account the correlation structure between subbands by modeling the wavelet coefficients through multivariate probability distributions. Two types of dependence are investigated in this paper: inter-scale dependence and inter-orientation dependence. The first is to model the dependence between the scales of the same orientation, and, the second is to model the dependence between the orientations of the same scale. We show that the information residing in the correlation between subbands improve the accuracy of the change map. The multivariate Gaussian distribution (MGD) is a natural extension of the univariate Gaussian distribution (GD). Indeed, the Gaussian distribution (GD) gives a quite good approximation of the probability distributions of a small region (a sliding window) [26] and when some Gaussianity are introduced into the data when the images were re-sampled and filtered. Moreover, MGD can be used to model wavelet coefficient magnitudes and correlation between subbands. In addition, a closed-form expression exists for the KLD between two MGDs.

The paper is organized as follows. In section II, we introduce two multivariate statistical models used for our study. They model the inter-scale and the inter-orientation dependence. Change detection using Kullback-Leibler divergence are presented in section III, where the former is calculated for the two cases cited before. Real data used for evaluation and experimental setting are described in section IV. Finally, the discussion, and some concluding remarks close up this paper.

II. Statistical modeling in Wavelet domain

In this section, a multivariate Gaussian distribution referred as MGD is used. A sliding window manner is applied for change detection and the wavelet transform is applied in each window producing multiscale oriented subbands. The general framework of the proposed method is shown in Fig. 1.

A. Inter-scale dependence

After wavelet decomposition, we have $4L$ sub-images where L is the number of scales. These sub-images are represented at this stage by $\boldsymbol{\mathcal{X}^i} = \{\boldsymbol{H^i}, \boldsymbol{V^i}, \boldsymbol{D^i}, \boldsymbol{A^i}\}$ where $i \in \{1,2\}$ and $\boldsymbol{H^i} = (H_1^i, H_2^i, ..., H_L^i)^t$, $\boldsymbol{V^i} = (V_1^i, V_2^i, ..., V_L^i)^t$, $\boldsymbol{D^i} = (D_1^i, D_2^i, ..., D_L^i)^t$, $\boldsymbol{A^i} = (A_1^i, A_2^i, ..., A_L^i)^t$ are L-dimensional random vectors representing the sub-image horizontal, vertical, diagonal details and approximations, respectively, and are distributed according MGDs. The corresponding $L \times L$ covariance matrices of the previous random vectors are $\boldsymbol{\Sigma_H^i}$, $\boldsymbol{\Sigma_V^i}$, $\boldsymbol{\Sigma_D^i}$ and $\boldsymbol{\Sigma_A^i}$, respectively, and are estimated from sub-images to quantify the dependence between scales.

B. Inter-orientation dependence

To measure the inter-orientation dependence, we constitute a new set of vectors $\boldsymbol{\mathcal{Y}^i} = \{\boldsymbol{Y_1^i}, \boldsymbol{Y_2^i}, ..., \boldsymbol{Y_L^i}\}$ where $i \in \{1,2\}$ and $\boldsymbol{Y_j^i} = (A_j^i, H_j^i, V_j^i, D_j^i)^t$ are 4-dimensional random vectors composed by variables representing the sub-image horizontal, vertical, diagonal details and approximations, respectively, at the scale j where $j \in \{1, 2, ..., L\}$ and $\boldsymbol{Y_j^i}$ are distributed according to MGDs. To measure the dependence between orientations of the same scale, the 4×4 covariance matrices are estimated for each scale from sub-images.

III. Change Detection Based On Kullback-Leibler in wavelet domain

A. Kullback-Leibler divergence

To quantify a change detection between two acquisition dates we need to analyze the modification of the statistics of each pixel's neighborhood. Several approaches can be taken: the mean square error between the two distribution, the norm of a vector of moments, etc [26]. In our study, we choose to use the Symmetric Kullback-Leibler distance as a similarity measure since it is a good similarity indicator for change detection [21]. If the statistics of the two sliding windows are the same the symmetric Kullback-Leibler distance is small. Let X^1 and X^2 be two random variables with probability density functions f_{X^1} and f_{X^2}. The KLD from X^2 to X^1 is given by

$$KL(X^2||X^1) = \int \log\left(\frac{f_{X^1}(x)}{f_{X^2}(x)}\right) f_{X^1}(x)dx, \qquad (1)$$

The symmetric KL similarity measure between X^1 and X^2 is

$$KL(X^1, X^2) = KL(X^2||X^1) + KL(X^1||X^2). \qquad (2)$$

If the X^1 and X^2 are distributed according to a GD with mean μ_1 and μ_2 and variance σ_1 and σ_2, respectively, the symmetric version of the KLD has the following form

$$KL(X^1, X^2) = \frac{\sigma_1^4 + \sigma_2^4 + (\mu_1 - \mu_2)^2(\sigma_1^2 + \sigma_2^2)}{2\sigma_1^2\sigma_2^2} \qquad (3)$$

If $\boldsymbol{X^1}$ and $\boldsymbol{X^2}$ are two random k-vectors with joint density functions $f_{\boldsymbol{X^1}}$ and $f_{\boldsymbol{X^2}}$, respectively, and are distributed according to the MGD with k-dimensional mean vector $\boldsymbol{\mu_1}$

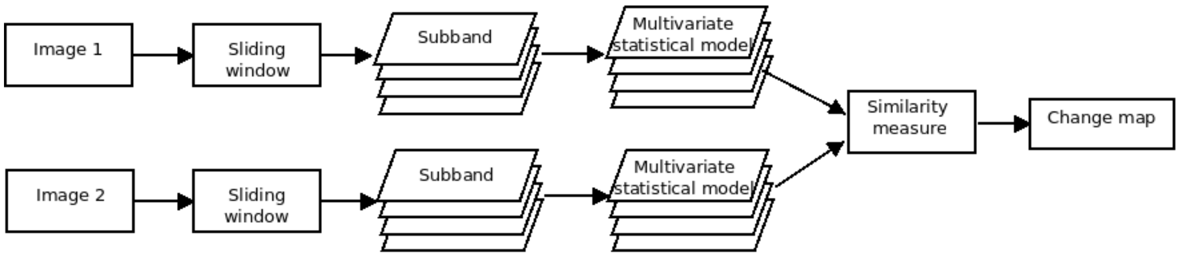

Fig. 1: Proposed method for SAR change detection in wavelet domain. The wavelet transform decomposes a sliding window into multiple subbands. The subband coefficients are combined to form different vectors for the study of inter-scale and inter-orientation dependences. KLD between pdfs of multivariate distributions is used to generate a change map.

and $\boldsymbol{\mu_2}$ and $k \times k$ covariance matrix $\boldsymbol{\Sigma_1}$ and $\boldsymbol{\Sigma_2}$, then the symmetric version of the KLD has the following form

$$\begin{aligned} KL(\boldsymbol{X^1}, \boldsymbol{X^2}) = \frac{1}{2} \big[& tr({\boldsymbol{\Sigma_2}}^{-1}\boldsymbol{\Sigma_1} + {\boldsymbol{\Sigma_1}}^{-1}\boldsymbol{\Sigma_2}) - 2k \\ & + (\boldsymbol{\mu_2} - \boldsymbol{\mu_1})^t ({\boldsymbol{\Sigma_2}}^{-1} + {\boldsymbol{\Sigma_1}}^{-1})(\boldsymbol{\mu_2} - \boldsymbol{\mu_1}) \big] \end{aligned} \tag{4}$$

B. KLD for the inter-scale dependence

The symmetric KLD of two sliding windows is defined as the sum of similarity measures of each L-vector of the same orientation

$$\begin{aligned} KL(\boldsymbol{\mathcal{X}^1}, \boldsymbol{\mathcal{X}^2}) = & KL(\boldsymbol{H^1}, \boldsymbol{H^2}) + KL(\boldsymbol{V^1}, \boldsymbol{V^2}) \\ & + KL(\boldsymbol{D^1}, \boldsymbol{D^2}) + KL(\boldsymbol{A^1}, \boldsymbol{A^2}) \end{aligned} \tag{5}$$

Where $KL(\boldsymbol{H^1}, \boldsymbol{H^2})$, $KL(\boldsymbol{D^1}, \boldsymbol{D^2})$, $KL(\boldsymbol{V^1}, \boldsymbol{V^2})$ and $KL(\boldsymbol{A^1}, \boldsymbol{A^2})$ are calculated using the (4). In the case of the subbands are assumed independent, the total similarity of two blocks or two sliding windows are defined as

$$\begin{aligned} KL(\boldsymbol{\mathcal{X}^1}, \boldsymbol{\mathcal{X}^2}) = & \sum_{j=1}^{L} KL(H_j^1, H_j^2) + KL(D_j^1, D_j^2) \\ & + KL(V_j^1, V_j^2) + KL(A_j^1, A_j^2) \end{aligned} \tag{6}$$

Where $KL(H_j^1, H_j^2)$, $KL(D_j^1, D_j^2)$, $KL(V_j^1, V_j^2)$ and $KL(A_j^1, A_j^2)$ are calculated using (3)

C. KLD for the inter-orientation dependence

The symmetric KLD of two sliding windows is defined as the sum of similarity measures of each 4-vector of the same scale

$$KL(\boldsymbol{\mathcal{Y}^1}, \boldsymbol{\mathcal{Y}^2}) = \sum_{j=1}^{L} KL(\boldsymbol{Y_j^1}, \boldsymbol{Y_j^2}) \tag{7}$$

In the case of the orientations of the same scale are assumed independent, the total similarity of two sliding windows are defined also by Eq. (6).

D. Total KLD

The total similarity of two blocks or two sliding windows are defined as the sum of similarity measures of (5) and (7)

$$KL = \frac{1}{2} \left(KL(\boldsymbol{\mathcal{X}^1}, \boldsymbol{\mathcal{X}^2}) + KL(\boldsymbol{\mathcal{Y}^1}, \boldsymbol{\mathcal{Y}^2}) \right) \tag{8}$$

IV. Experimental results and discussion

A. Experiments with real data

To evaluate our proposed method, a pair of Radarsat images acquired before and after the eruption of the Nyiragongo volcano are used in this study. The volcano occurred in January 2002. In Fig.(2), we show two images before (a) and after change (b) and a binary change map (c) produced using ground measures [26]. It is worth noticing that these images have undergone a series of image pre-processing such as filtering, re-sampling, causing the modification of the local statistics of the image. The ground truth data in Fig.(2).c is not perfect due to the presence of a severe mis-registration caused by the lack of a proper digital terrain model [26].

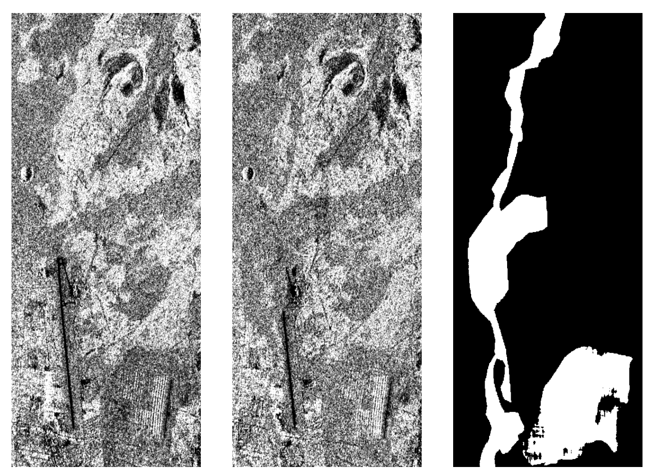

(a) (b) (c)

Fig. 2: Data and ground truth for the Nyiragongo volcanic eruption of January 2002.

To obtain reliable results, a sliding window with size $\{24, 32, 40, 48\}$ is used for the input images (before and after change). Each of these sliding windows is decomposed into $L = (1, 2, 3)$ scales using discrete undecimated stationary wavelet transform (SWT) with a Daubechies filter bank (db1, db2, db3, db4). For the sake of comparison, two models with and without dependency are used in this study. The first model is defined by (8) and based on the MGD, and the second model is based on (6) and depends on GD. The GD and MGD are estimated with different window sizes. To evaluate the accuracy of the change map independent of the thresholding algorithm, the receiver operating characteristic (ROC) curve is used and the area under ROC curve (AUC) is computed as a performance measure. The ROC curve is the evolution of the true positive rate (TPR) as function of false positive rate (FPR) [21]. The area under curve (AUC) is a good indicator of change. The larger the area the better the performance [21].

B. Results

The area under the ROC curve are shown in Table I. At each window size, the best and the worst values are highlighted in red and green, respectively. From this table, we can draw the following general conclusions. First, it can be clearly seen that multivariate distribution given by MGD provides better performance than univariate distribution as the GD for any window sizes, any scales and any filters. Second, we can see that as the window size increases, the AUC always increases. For a fixed window size, the AUC increases as the number of scales increases. This can be explained by the fact that the information residing in the dependence between subbands improves the accuracy of the change map and than can better characterized by a multivariate statistical model than an univariate statistical model. We have also the following particular notes. For a fixed window size and scale, the AUC for MGDs and GDs decrease as the order of the filters increases. This is explained due to the fact that the correlation between the wavelet subbands decreases as the filter order increases. Based on this table, we conclude that the best window size and the best scale are 48×48 and $L = 3$, respectively. For illustrative purposes, the change detection image corresponding to the calculation of the total KL divergence given by (8) is presented in Fig.3 for a window size of 48×48 and a scale value $L = 3$.

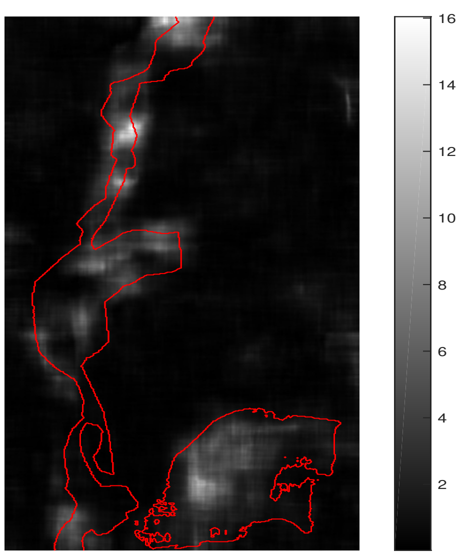

Fig. 3: Total KL computed using Eq. (8) of the change detection image.

Scale	Method	dbn	24	32	40	48
1	MGD	db1	0.7947	0.8265	0.8395	0.8399
		db2	0.7938	0.8252	0.8382	0.8386
		db3	0.7929	0.8242	0.8380	0.8379
		db4	0.7923	0.8234	0.8379	0.8366
	GD	db1	0.7843	0.8152	0.8281	0.8287
		db2	0.7833	0.8149	0.8277	0.8279
		db3	0.7826	0.8140	0.8262	0.8266
		db4	0.7820	0.8133	0.8281	0.8254
2	MGD	db1	0.7942	0.8267	0.8416	0.8494
		db2	0.7939	0.8256	0.8405	0.8489
		db3	0.7944	0.8251	0.8398	0.8482
		db4	0.7948	0.8256	0.8396	0.8477
	GD	db1	0.7846	0.8164	0.8310	0.8391
		db2	0.7835	0.8153	0.8302	0.8384
		db3	0.7828	0.8145	0.8296	0.8378
		db4	0.7822	0.8138	0.8291	0.8374
3	MGD	db1	0.8071	0.8407	0.8485	0.8591
		db2	0.8038	0.8419	0.8494	0.8606
		db3	0.7987	0.8404	0.8501	0.8617
		db4	0.7977	0.8374	0.8487	0.8621
	GD	db1	0.7906	0.8265	0.8359	0.8473
		db2	0.7894	0.8262	0.8348	0.8469
		db3	0.7883	0.8259	0.8338	0.8466
		db4	0.7875	0.8257	0.8329	0.8463

TABLE I: The Area Under Curve (AUC) for different window sizes and different scales are measured for MGD and GD. The best values are marked by red color and the worst by green color.

V. Discussion and Conclusion

In this paper, a method for SAR change detection in wavelet domain is proposed. It is based on MGD for modeling the coefficient magnitude of the wavelet subbands. It takes into account the dependency between subbands such as the inter-scale dependence and inter-orientation dependence. Wavelet transform is used to decompose the image into multiple scales and orientations. The total Kullback-Leibler divergence is the sum of the Kullback-Leibler of the inter-scale and inter-orientation dependence. Our approach is evaluated using different window sizes and different scales compared with the univariate GD. Through the study, the MGD in wavelet domain shows promising results since it takes into account the correlation between subband comparing to the conventional approach as the univariate Gaussian distribution. Although the method performs slightly better than the conventional approach, improvement can be achieved, first, by including other multivariate distributions as the multivariate generalized Gaussian distribution. Second, by extending the study to polarimetric SAR (PolSAR) data to exploit the joint modeling of the polarization channel correlation. We expect that these additional data will enhance the change detection task. Finally, by adding a third type of correlation: the inter-polarization dependence, in order to use the information embedded in the correlation between the polarization channels.

References

[1] R. Almeida-Filho, A. Rosenqvist, Y. E. Shimabukuro, and R. Silva-Gomez, "Detecting deforestation with multitemporal L-band SAR imagery: a case study in western brazilian amazônia," *International Journal of Remote Sensing*, vol. 28, no. 6, pp. 1383–1390, 2007.

[2] O. Yuzugullu, E. Erten, and I. Hajnsek, "Rice growth monitoring by means of X-band co-polar SAR: Feature clustering and BBCH scale," *IEEE Geoscience and Remote Sensing Letters*, vol. 12, no. 6, pp. 1218–1222, 2015.

[3] S. Stramondo, C. Bignami, M. Chini, N. Pierdicca, and A. Tertulliani, "Satellite radar and optical remote sensing for earthquake damage detection: results from different case studies," *International Journal of Remote Sensing*, vol. 27, no. 20, pp. 4433–4447, 2006.

[4] D.-j. Kim, S. Hensley, S.-H. Yun, and M. Neumann, "Detection of durable and permanent changes in urban areas using multitemporal polarimetric UAVSAR data," *IEEE Geoscience and Remote Sensing Letters*, vol. 13, no. 2, pp. 267–271, 2016.

[5] S. C. Steele-Dunne, H. McNairn, A. Monsivais-Huertero, J. Judge, P.-W. Liu, and K. Papathanassiou, "Radar remote sensing of agricultural canopies: A review," *IEEE Journal of Selected Topics in Applied Earth Observations and Remote Sensing*, vol. 10, no. 5, pp. 2249–2273, 2017.

[6] H. McNairn, X. Jiao, A. Pacheco, A. Sinha, W. Tan, and Y. Li, "Estimating canola phenology using synthetic aperture radar," *Remote Sensing of Environment*, vol. 219, pp. 196–205, 2018.

[7] V. Akbari, S. Solberg, and S. Puliti, "Multitemporal Sentinel-1 and Sentinel-2 images for characterization and discrimination of young forest stands under regeneration in norway," *IEEE Journal of Selected Topics in Applied Earth Observations and Remote Sensing*, vol. 14, pp. 5049–5063, 2021.

[8] V. Akbari, S. N. Anfinsen, A. P. Doulgeris, T. Eltoft, G. Moser, and S. B. Serpico, "Polarimetric SAR change detection with the complex hotelling–lawley trace statistic," *IEEE Transactions on Geoscience and Remote Sensing*, vol. 54, no. 7, pp. 3953–3966, 2016.

[9] N. Bouhlel, V. Akbari, and S. Méric, "Change detection in multilook polarimetric SAR imagery with determinant ratio test statistic," *IEEE Transactions on Geoscience and Remote Sensing*, vol. 60, pp. 1–15, 2022.

[10] S. Hachicha and F. Chaabane, "Multi-temporal SAR change detection an monitoring," in *International Archives of the Photogrammetry, Remote Sensing and Spatial Information Sciences*, September 2011, pp. 293–298.

[11] E. Rignot and J. van Zyl, "Change detection techniques for ers-1 SAR data," *Geoscience and Remote Sensing, IEEE Transactions on*, vol. 31, no. 4, pp. 896–906, Jul 1993.

[12] Y. Bazi, L. Bruzzone, and F. Melgani, "An unsupervised approach based on the generalized gaussian model to automatic change detection in multitemporal SAR images," *Geoscience and Remote Sensing, IEEE Transactions on*, vol. 43, no. 4, pp. 874–887, April 2005.

[13] B. Hou, Q. Wei, Y. Zheng, and S. Wang, "Unsupervised change detection in SAR image based on gauss-log ratio image fusion and compressed projection," *Selected Topics in Applied Earth Observations and Remote Sensing, IEEE Journal of*, vol. 7, no. 8, pp. 3297–3317, Aug 2014.

[14] A. Atto, E. Trouve, Y. Berthoumieu, and G. Mercier, "Multidate divergence matrices for the analysis of SAR image time series," *Geoscience and Remote Sensing, IEEE Transactions on*, vol. 51, no. 4, pp. 1922–1938, April 2013.

[15] N. Bouhlel and S. Méric, "Multilook polarimetric SAR change detection using stochastic distances between matrix-variate $\mathcal{G}_d^0$ distributions," *IEEE Transactions on Geoscience and Remote Sensing*, vol. 58, no. 10, pp. 6823–6843, 2020.

[16] J. R. Bunch and R. D. Fierro, "A constant-false-alarm-rate algorithm," *Linear Algebra and its Applications*, vol. 172, pp. 231 – 241, 1992.

[17] N. Otsu, "A threshold selection method from gray-level histograms," *IEEE Transactions on Systems, Man, and Cybernetics*, vol. 9, no. 1, pp. 62–66, Jan 1979.

[18] M. Ghanbari and V. Akbari, "Unsupervised change detection in polarimetric SAR data with the hotelling-lawley trace statistic and minimum-error thresholding," *IEEE Journal of Selected Topics in Applied Earth Observations and Remote Sensing*, vol. 11, no. 12, pp. 4551–4562, Dec 2018.

[19] M. Kivanc Mihcak, I. Kozintsev, K. Ramchandran, and P. Moulin, "Low-complexity image denoising based on statistical modeling of wavelet coefficients," *Signal Processing Letters, IEEE*, vol. 6, no. 12, pp. 300–303, Dec 1999.

[20] S. Choy and C. Tong, "Statistical wavelet subband characterization based on generalized gamma density and its application in texture retrieval," *Image Processing, IEEE Transactions on*, vol. 19, no. 2, pp. 281–289, Feb 2010.

[21] S. Cui and M. Datcu, "Statistical wavelet subband modeling for multi-temporal SAR change detection," *Selected Topics in Applied Earth Observations and Remote Sensing, IEEE Journal of*, vol. 5, no. 4, pp. 1095–1109, Aug 2012.

[22] M. Do and M. Vetterli, "Wavelet-based texture retrieval using generalized gaussian density and kullback-leibler distance," *Image Processing, IEEE Transactions on*, vol. 11, no. 2, pp. 146–158, Feb 2002.

[23] G. Verdoolaege, Y. Rosseel, M. Lambrechts, and P. Scheunders, "Wavelet-based colour texture retrieval using the kullback-leibler divergence between bivariate generalized gaussian models," in *Image Processing (ICIP), 2009 16th IEEE International Conference on*, Nov 2009, pp. 265–268.

[24] J. Huang, "Study on the correlation properties of wavelet transform coefficients and the applications in a neural network-based hybrid image coding system," in *presented at the CISST Las Vegas*, Jun 2003, pp. 22–26.

[25] G. Tzagkarakis, B. Beferull-Lozano, and P. Tsakalides, "Rotation-invariant texture retrieval with gaussianized steerable pyramids," *Image Processing, IEEE Transactions on*, vol. 15, no. 9, pp. 2702–2718, Sept 2006.

[26] J. Inglada and G. Mercier, "A new statistical similarity measure for change detection in multitemporal SAR images and its extension to multiscale change analysis," *Geoscience and Remote Sensing, IEEE Transactions on*, vol. 45, no. 5, pp. 1432–1445, May 2007.